

Tie-dyed1 and *Sucrose export defective1* act independently to promote carbohydrate export from maize leaves

Yi Ma · R. Frank Baker · Maria Magallanes-Lundback ·
Dean DellaPenna · David M. Braun

Received: 19 August 2007 / Accepted: 19 September 2007 / Published online: 9 October 2007
© Springer-Verlag 2007

Abstract *tie-dyed1* (*tdy1*) and *sucrose export defective1* (*sxd1*) are recessive maize (*Zea mays*) mutants with nonclonal chlorotic leaf sectors that hyperaccumulate starch and soluble sugars. In addition, both mutants display similar growth-related defects such as reduced plant height and inflorescence development due to the retention of carbohydrates in leaves. As *tdy1* and *sxd1* are the only variegated leaf mutants known to accumulate carbohydrates in any plant, we investigated whether *Tdy1* and *Sxd1* function in the same pathway. Using aniline blue staining for callose and transmission electron microscopy to inspect plasmodesmatal ultrastructure, we determined that *tdy1* does not have any physical blockage or alteration along the symplastic transport pathway as found in *sxd1* mutants. To test whether the two genes function in the same genetic pathway, we constructed F₂ families segregating both mutations. Double mutant plants showed an additive interaction for growth related phenotypes and soluble sugar accumulation, and expressed the leaf variegation pattern of both single mutants indicating that *Tdy1* and *Sxd1* act in separate genetic pathways. Although *sxd1* mutants lack tocopherols, we determined that *tdy1* mutants have wild-type tocopherol levels, indicating that *Tdy1* does not function in the same

biochemical pathway as *Sxd1*. From these and other data we conclude that *Tdy1* and *Sxd1* function independently to promote carbon export from leaves. Our genetic and cytological studies implicate *Tdy1* functioning in veins, and a model discussing possible functions of TDY1 is presented.

Keywords Carbohydrate accumulation · Carbon partitioning · Maize · *sucrose export defective1* · *tie-dyed1*

Introduction

Sugars synthesized in photosynthetic leaf cells must be transported into the veins for distribution to nonphotosynthetic tissues. Maize (*Zea mays*) is a C₄ plant which displays Kranz anatomy in its leaves (Esau 1977). Veins are surrounded by bundle sheath cells which in turn are surrounded by mesophyll cells. Mesophyll and bundle sheath cells cooperatively perform the reactions of photosynthesis and carbon assimilation. Sucrose is synthesized in the cytoplasm of mesophyll cells (Lunn and Furbank 1999), diffuses through plasmodesmata into bundle sheath cells, and then into vascular parenchyma cells (Russin et al. 1996). Maize is an apoplastic phloem loading species (Evert et al. 1978), whereby sucrose is exported from the vascular parenchyma cells to the apoplast by an unknown mechanism (see Lalonde et al. 2004 for discussion). Sucrose is then imported into phloem companion cells and/or sieve elements by sucrose transporters located in the plasma membrane (Aoki et al. 1999; Lalonde et al. 2004; Sauer 2007; Scofield et al. 2007). The energy to transport sucrose into the phloem is derived from H⁺-ATPases that generate the proton motive force across the plasma membrane (Bush 1993; Gaxiola et al. 2007). In addition, the abundance of the sucrose transporter that controls phloem

Electronic supplementary material The online version of this article (doi:10.1007/s00425-007-0636-6) contains supplementary material, which is available to authorized users.

Y. Ma · R. F. Baker · D. M. Braun (✉)
Department of Biology, Pennsylvania State University,
University Park, PA 16802, USA
e-mail: dbraun@psu.edu

M. Magallanes-Lundback · D. DellaPenna
Department of Biochemistry and Molecular Biology,
Michigan State University, East Lansing, MI 48824, USA

loading is transcriptionally regulated by a sucrose-sensing signal transduction pathway (Chiou and Bush 1998; Vaughn et al. 2002; Ransom-Hodgkins et al. 2003). If carbon transport into the vein is blocked, carbohydrates accumulate in the photosynthetic cells, leading to down-regulation of photosynthetic gene expression and reduced chlorophyll levels (chlorosis) (Sheen 1990; Goldschmidt and Huber 1992; Riesmeier et al. 1994; Krapp and Stitt 1995; Burkle et al. 1998; Gottwald et al. 2000; Jeannette et al. 2000). Even though the transport pathway for assimilated carbon has been studied in maize leaves for almost 40 years (Hofstra and Nelson 1969), the mechanisms that regulate sucrose export from leaves remain poorly understood.

To date, two recessive maize mutants have been described with defects in carbon export from leaves. *tiedyed1* (*tdy1*) and *sucrose export defective1* (*sxd1*) mutants develop nonclonal chlorotic leaf sectors that hyperaccumulate starch and soluble sugars (Russin et al. 1996; Provencher et al. 2001; Braun et al. 2006). Other mutants with variegated leaves have been characterized, but none have carbohydrate accumulation within the chlorotic regions (Rhoades and Carvalho 1944; Fisher and Eschrich 1985; Madore 1990; Yu et al. 2007). *tdy1* and *sxd1* both display growth-related defects such as reduced plant height and inflorescence development due to the retention of carbohydrates in leaf tissues. However, their phenotypes also show significant differences. *sxd1* mutant leaves progressively exhibit chlorosis which initiates at the leaf tip and basipetally spreads toward the base. Interestingly, in *sxd1* mutants, only the leaf minor veins are affected in phloem loading (Russin et al. 1996). The *tdy1* mutant phenotype is distinct from *sxd1* mutants in that large chlorotic regions develop throughout leaf blade tissue. Further, *tdy1* chlorotic regions form only during a limited time as the leaf emerges from the whorl and, once formed, do not expand (Braun et al. 2006). Lastly, in *tdy1* mutants, chlorotic tissues are often bounded by lateral veins, implicating this vein class in limiting the expansion of a *tdy1* chlorotic sector (Baker and Braun 2007).

Sxd1 encodes tocopherol cyclase, an enzyme functioning in tocopherol (vitamin E) biosynthesis, and *sxd1* mutants lack tocopherols (Sattler et al. 2003). Absence of tocopherols results in callose deposition over the plasmodesmata at the bundle sheath-vascular parenchyma cell interface of leaf minor veins (Russin et al. 1996; Botha et al. 2000; Provencher et al. 2001). This occludes these passageways and prevents sucrose from moving into the vein, resulting in the build-up of carbohydrates in photosynthetic cells. The function of tocopherols in preventing callose deposition in the phloem is evolutionarily conserved. RNAi-mediated suppression of tocopherol cyclase activity in potato results in callose deposition in vascular-associated cells and carbohydrate accumulation in the photosynthetic cells

(Hofius et al. 2004). In addition, in *Arabidopsis* tocopherol cyclase mutants and other vitamin E deficient mutants, callose is deposited in phloem parenchyma transfer cells and the photosynthetic cells accumulate carbohydrates if the plants are subjected to nonfreezing low temperatures (Maeda et al. 2006). It is not known how lack of tocopherols causes callose deposition.

Because both mutants show defects in carbon export from leaves, we examined whether *Tdy1* and *Sxd1* function in the same pathway to limit leaf carbohydrate accumulation. Using aniline blue fluorescence microscopy and transmission electron microscopy (TEM) we determined that carbohydrate accumulation in *tdy1* mutant leaves does not result from a similar impediment to phloem loading as in *sxd1* mutants. To genetically test whether the two genes function in the same pathway, we analyzed F₂ families segregating both mutations. We observed that the double mutant plants showed an additive interaction for growth-related phenotypes and soluble sugar accumulation indicating that the two genes function in separate genetic pathways. To determine if *Tdy1* functions in the same biochemical pathway as *Sxd1*, we measured tocopherol levels in mutant plants. We found that *tdy1* mutants contain wild-type levels of tocopherols, indicating that *Tdy1* does not function in the same biochemical process as *Sxd1*. Thus, from the combination of cellular, genetic and biochemical investigations we conclude that *Tdy1* and *Sxd1* function independently to promote carbon export from leaves. Additionally, genetic and cytological studies suggest that *Tdy1* functions within the veins, and a model of possible TDY1 functions is discussed.

Materials and methods

Plant materials

Plants were grown in the summer in the Rock Springs Agronomy Farm, Pennsylvania State University, and in the winter in Juana Diaz, Puerto Rico. The *tdy1-Reference* (*tdy1-R*) (Braun et al. 2006) and *sxd1-1* (Russin et al. 1996) mutations were backcrossed to the B73 inbred line five times prior to crossing together. F₂ families were generated by crossing *tdy1-R* and *sxd1-1* mutant plants and self-pollinating the F₁ individuals.

Morphological analyses

Plant height was measured from the soil surface to the tip of the central spike of the tassel. Tassel length was measured from the node of the flag leaf to the tip of the central spike. Anthesis was recorded as the day of first pollen shed. Plants were scored as having produced ears if either (1) ears were clearly visible, (2) silks were visible emerging from the leaf

sheath, or (3) ears developed such that they were identifiable by peeling back the ear leaf sheath. For wild-type and *tdy1-R* single mutants $n = 18$ for all measurements. For *sxd1-1* single mutants, 12 of the 16 plants produced a tassel that shed pollen, and 13 produced an ear. For *tdy1-R; sxd1-1* double mutants, 7 of the 15 plants shed pollen and 8 made an ear. Barren tassels that did not shed pollen were not included in the tassel length or anthesis measurements.

Aniline blue staining

Leaf strips 1 cm in width were cut from mutant and wild-type leaves. The abaxial epidermis and the mesophyll cells directly beneath it were gently scraped away with a single-edge razor to expose the inner leaf tissues. The leaf strip was placed on a slide, briefly stained with a 0.05% aniline blue and immediately viewed using a 360–370-nm excitation filter and a 420-nm long pass emission filter on a Nikon Eclipse 80i fluorescent microscope. Epifluorescent illumination was provided by a 100-W mercury lamp, and images were recorded using a DXM1200F Nikon digital camera.

TEM analyses

For tissue fixation, leaf samples were diced into 3×1 mm pieces, placed in 4% glutaraldehyde, 1% paraformaldehyde, 0.3% Tween 20, 50 mM sodium cacodylate, pH 7.4, and vacuum infiltrated on ice for 4–6 h. Samples were post-fixed in 1–2% osmium tetroxide at 4°C overnight, subsequently dehydrated through a graded acetone series and embedded in Spurr's epoxy resin (Spurr 1969). Thin sections (90–100 nm) were cut on a Leica Ultracut E ultramicrotome with a glass knife and lifted onto 200-mesh copper grids. The grids were stained in 2% uranyl acetate, followed by Reynold's lead citrate and observed with a JEOL JEM 1200 EXII at an accelerating voltage of 80 kV.

Chlorophyll quantification

Relative levels of total chlorophylls were quantified from leaves using a SPAD 502 Data Logger Chlorophyll Meter (Spectrum Technologies). For each tissue, 30 samples were measured, and the experiment was performed three times. Representative data from one replicate are shown.

Sugars and starch quantification

Leaf tissues were collected at the end of the photoperiod, weighed and frozen at -80°C . Carbohydrate extraction was performed according to Dinges et al. (2001). Sugars and starch were quantified using commercial assay kits according to the manufacturer's instructions (R-Biopharm). Six samples from each tissue type were measured in triplicate.

For visualizing starch in leaves, samples were collected at the end the photoperiod, decolorized by boiling in 95% ethanol and stained with iodine-potassium iodide (IKI) (Ruzin 1999).

Tocopherol quantification

Leaf discs of 11 mm were harvested with a cork borer from leaf tissues, weighed and immediately frozen on dry ice. Total lipids were extracted from collected tissues and tocopherols measured according to (Sattler et al. 2003).

Results

tdy1-R and *sxd1-1* single mutants both display variegated chlorotic leaves

tdy1-R and *sxd1-1* mutants show striking parallels in their leaf phenotypes. Both develop chlorotic sectors that hyperaccumulate starch and soluble sugars in leaf blades (Fig. 1). However, there are also distinctions. Whereas wild-type leaves have a uniform, dark green color, *sxd1-1* mutant leaves develop a chlorotic phenotype that shows a continuum of expression from strongest at the tip to mildest toward the base (Fig. 1a, b). In addition, at the tip and leaf margins, the chlorotic tissues progressively accumulate anthocyanin and excess starch (Fig. 1b, e). In *sxd1-1* leaves, no clear, delineated boundaries occur between green and chlorotic regions. Conversely, *tdy1-R* mutants display a variegated pattern of chlorotic and normal appearing green regions throughout leaf blade tissue (Fig. 1c). Additionally, the boundaries between *tdy1-R* chlorotic and normal appearing green tissue are sharp and distinct, and they tend to occur at lateral veins (Baker and Braun 2007). As in *sxd1-1* mutants, chlorotic regions in *tdy1-R* mutants hyperaccumulate starch relative to green tissues (Fig. 1f). *tdy1* and *sxd1* are the only known leaf variegation mutants that hyperaccumulate carbohydrates in any plant; therefore, we investigated whether *Tdy1* and *Sxd1* function in a common pathway influencing carbon partitioning in leaves.

Carbohydrate accumulation in *tdy1-R* mutants occurs by a different mechanism than in *sxd1-1* plants

To address whether the two genes function in the same pathway, we investigated if the mechanism for carbohydrate accumulation was similar in the two mutants. Carbohydrate accumulation in *sxd1-1* mutants results from a blockage in the symplastic pathway of sucrose movement (Russin et al. 1996; Botha et al. 2000; Provencher et al. 2001). Specifically, at the bundle sheath–vascular parenchyma cell interface of leaf minor veins, callose is deposited

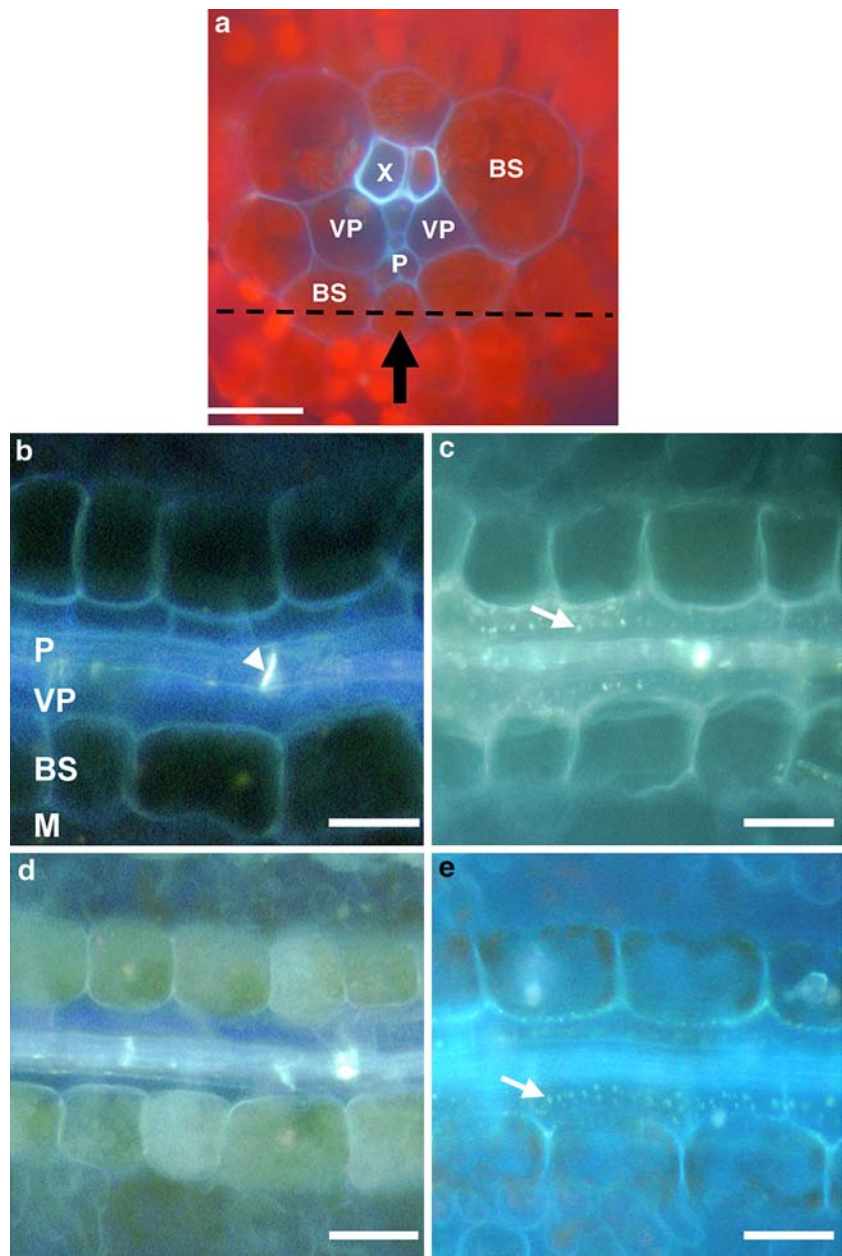
Fig. 1 *tdy1-R* and *sxd1-1* leaves display chlorotic sectors that hyperaccumulate carbohydrates. **a** Wild-type leaf showing uniform dark green color. **b** *sxd1-1* mutant leaf displaying a chlorotic gradient, strongest at the tip to mildest toward the leaf base. Anthocyanins accumulate in the chlorotic tissues at the leaf tip and margins. **c** *tdy1-R* mutant leaf containing variegated chlorotic and green sectors throughout the leaf blade. **d–f** Cleared, IKI stained leaf tissues showing that mutant chlorotic regions hyperaccumulate starch. **d** Wild type. **e** *sxd1-1*. **f** *tdy1-R*. Scale bars represent 4 cm



over the plasmodesmata in bundle sheath cells. This blockage prevents sucrose from being loaded into the phloem and results in carbohydrate accumulation in the photosynthetic cells. To determine if the *tdy1-R* leaf phenotype is similarly caused by callose deposits plugging the plasmodesmata, we performed aniline blue staining and fluorescence microscopy. Aniline blue binds callose and fluoresces a blue–white color under UV light. In wild-type plants, only the sieve plates in the end walls of phloem sieve elements stain positively for callose (Fig. 2b). As previously reported, *sxd1-1* mutants display many punctate callose deposits at the vascular parenchyma–bundle sheath cell interface of minor veins (Fig. 2c) (Botha et al. 2000). In *tdy1-R* chlorotic regions, no ectopic callose deposits were detected at this interface (Fig. 2d). Further, no callose deposits were observed in any cells of minor or lateral veins in *tdy1-R* chlorotic tissues, nor in any cells of *tdy1-R* green regions (data not shown). These data suggest that *tdy1-R* mutants do not accumulate carbohydrates due to callose blocking symplastic sucrose movement.

Although we did not observe ectopic callose deposition in any cells in *tdy1-R* mutant leaves using aniline blue staining, it is possible that symplastic sucrose transport is precluded due to a different defect in plasmodesmal structure. To investigate this possibility, we performed TEM to inspect the plasmodesmata ultrastructure along the symplastic pathway. In minor veins from wild-type leaves, the plasmodesmata between bundle sheath and vascular parenchyma cells were unobstructed, spanned the cell wall and connected the cytoplasm between the two cells (Fig. 3a). Consistent with previous reports, minor veins from leaf tips expressing the *sxd1-1* mutant phenotype showed occlusions over the plasmodesmata on the bundle sheath cell side of the bundle sheath–vascular parenchyma cell interface (Fig. 3b) (Russin et al. 1996; Botha et al. 2000; Provencher et al. 2001). In *tdy1-R* mutant leaves, we found no occlusions over the plasmodesmata or alterations in their structure between the bundle sheath and vascular parenchyma cells in minor veins (Fig. 3c). In examining plasmodesmata along the symplastic pathway at all cellular interfaces in

Fig. 2 Aniline blue staining of ectopic callose deposits in leaf minor veins. **a** Cross section of a wild-type minor vein shown by UV autofluorescence indicating the cell types and orientation of view (*arrow*) for **b–e**. Abaxial cells were removed below the *black dotted line* to view the bundle sheath–vascular parenchyma cell interface. *X* xylem, *P* phloem, *VP* vascular parenchyma, *BS* bundle sheath, *M* mesophyll. **b–e** Aniline blue fluorescence images of paradermal sections along minor veins. **b** Wild-type cells lack punctate callose deposits indicating no blockages along the symplastic pathway. The bright fluorescence observed in the phloem corresponds to sieve plates (*arrowhead*). **c** *sxd1-1* minor veins contain many callose deposits at the bundle sheath–vascular parenchyma cell interface (*arrow*). **d** *tdy1-R* chlorotic tissue lacks callose deposition over plasmodesmata in any cells. **e** *tdy1-R; sxd1-1* double mutants contain callose deposits (*arrow*) at the bundle sheath–vascular parenchyma cell interface comparable to the level seen in *sxd1-1* single mutants. *Scale bar in a* represents 50 μ m, and in **b–e** 10 μ m



tdy1-R leaves, we did not observe any structural perturbations or occlusions (Fig. 3e–j). These data indicate that carbohydrate retention in *tdy1-R* mutant leaves does not appear to result from physical blockage or plasmodesmatal structural changes. Together, the aniline blue staining and TEM studies indicate that the cellular basis for the *tdy1-R* and *sxd1-1* phenotypes is different.

Double mutant plants show more severe growth defects than either single mutant

Both *tdy1-R* and *sxd1-1* single mutant plants have growth-related defects due to the retention of carbohydrates in leaves. To determine whether the two genes function in the

same genetic pathway promoting carbon export from leaves, we created F₂ families segregating both mutations. Both mutations are recessive and the F₂ segregation ratio fits the expected 9:3:3:1 prediction, indicating that neither mutant shows epistasis (Table 1). *sxd1-1* is a molecular null allele lacking transcripts (Provencher et al. 2001), and based on dosage analysis, *tdy1-R* is a genetic null allele (Braun et al. 2006). If *Tdy1* and *Sxd1* act in a linear genetic pathway, we would expect that the phenotype of the double mutant would be similar to one or the other mutant. If the two genes function in separate pathways, then we predict that the double mutant would be more severe than either single mutant.

To examine the interactions between *tdy1-R* and *sxd1-1*, we quantified the growth parameters of plant height, tassel

Fig. 3 TEM images of cellular interfaces along the symplastic pathway of minor veins. **a–d** Bundle sheath–vascular parenchyma cells. *Arrows* indicate the location of the plasma membrane in the bundle sheath cell. **a** Wild-type plasmodesmata span the cell wall, lack occlusions, and connect with the plasma membrane. **b** *sxd1-1* chlorotic leaf tips contain occlusions over the plasmodesmata on the bundle sheath cell side of the cell wall. **c** *tdy1-R* chlorotic sectors contain normal appearing plasmodesmata that lack occlusions. Note the plasmodesmata span the cell wall and connect with the plasma membrane. **d** *tdy1-R; sxd1-1* double mutant chlorotic tissues contain deposits over the plasmodesmata in the bundle sheath cell similar to *sxd1-1* single mutants. Additional cellular interfaces along the symplastic pathway of wild type (**e, g, i**) and *tdy1-R* chlorotic tissues (**f, h, j**) are shown. In **e–j** the plasmodesmata spanned the cell wall connecting the cytoplasms of adjacent cells and lacked occlusions. **e, f** BS–BS cells, **g, h** BS–M cells, **i, j** M–M cells. *BS* bundle sheath, *M* mesophyll. *Scale bars* represent 200 nm

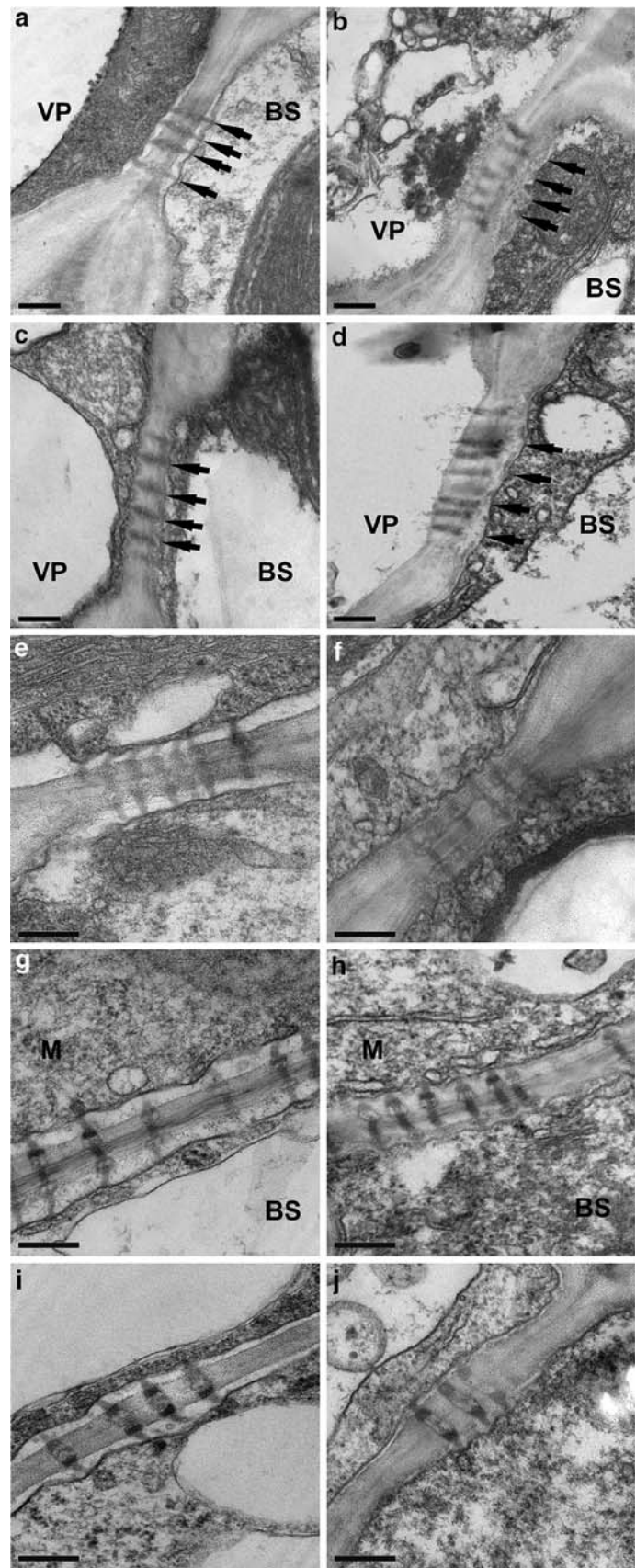


Table 1 Genetic segregation in F₂ families

Family #	Total	Wild type	<i>tdy1-R</i>	<i>sxd1-1</i>	<i>tdy1-R</i> ; <i>sxd1-1</i>	χ^2	<i>P</i>
DB 5503	93	48	22	16	7	2.0	<i>P</i> > 0.05
DB 5512	95	52	23	15	5	2.1	<i>P</i> > 0.05
DB 5523	93	55	18	15	5	0.6	<i>P</i> > 0.05
Total	281	155	63	46	17	2.9	<i>P</i> > 0.05

χ^2 analyses of *tdy1-R* and *sxd1-1* segregation in three F₂ families conform to a 9:3:3:1 expectation. Observed numbers of individuals are shown

size, time to anthesis and ear production (Fig. 4, Table 2). At the whole plant level, the double mutants express a more severe phenotype and show a stronger reduction in growth characteristics than either single mutant (Fig. 4a). Compared to wild-type, *tdy1-R* single mutants have an 11% decrease, *sxd1-1* mutants have a 24% reduction, and the *tdy1-R*; *sxd1-1* double mutant plants show the greatest reduction in plant height of 35.5%. Similar to plant height, tassel size is reduced 13% in *tdy1-R* plants, 29% in *sxd1-1* mutants, and 50% in *tdy1-R*; *sxd1-1* double mutants (Fig. 4c, Table 2). In addition, approximately half of the *tdy1-R*; *sxd1-1* double mutant plants produced very reduced tassel branches lacking spikelets (Fig. 4d). This phenotype was observed in 25% of the *sxd1-1* single mutants. Correlated with the tassel height defects, both mutations retarded time to flowering. Both *tdy1-R* and *sxd1-1* single mutants first shed pollen eight days later than wild-type siblings (Table 2). Double mutant plants were delayed even further by approximately another 5 days. Similarly, wild-type and *tdy1-R* mutant plants invariably made ears, and *sxd1-1* mutants produced ears 81% of the time. In contrast, only 53% of the double mutant plants produced an ear (Table 2). All of the growth defects observed in the single and double mutants are consistent with a restriction in assimilates transported to the growing portions of the plants. The double mutant plants showed the most severe phenotypes suggesting they have a greater reduction in carbohydrates exported out of leaves than in either single mutant. In support of this, the leaves of *tdy1-R*; *sxd1-1* double mutant plants are more strongly chlorotic than either single mutant, with a corresponding reduction in the amount of green tissue (compare Figs. 4b with 1b, c). In double mutant leaves, the tip to base gradient of chlorosis and anthocyanin pigmentation characteristic of the *sxd1-1* phenotype is superimposed on the *tdy1-R* chlorotic and green sector pattern. Double mutant leaves still contain some green tissues located at the leaf base as in *sxd1-1* single mutants; however, the boundaries between the chlorotic and green regions are sharp and distinct as in *tdy1-R* mutants (Fig. 4b). Thus, the double mutant leaves express the phenotypes of both single mutants, and double mutant plants

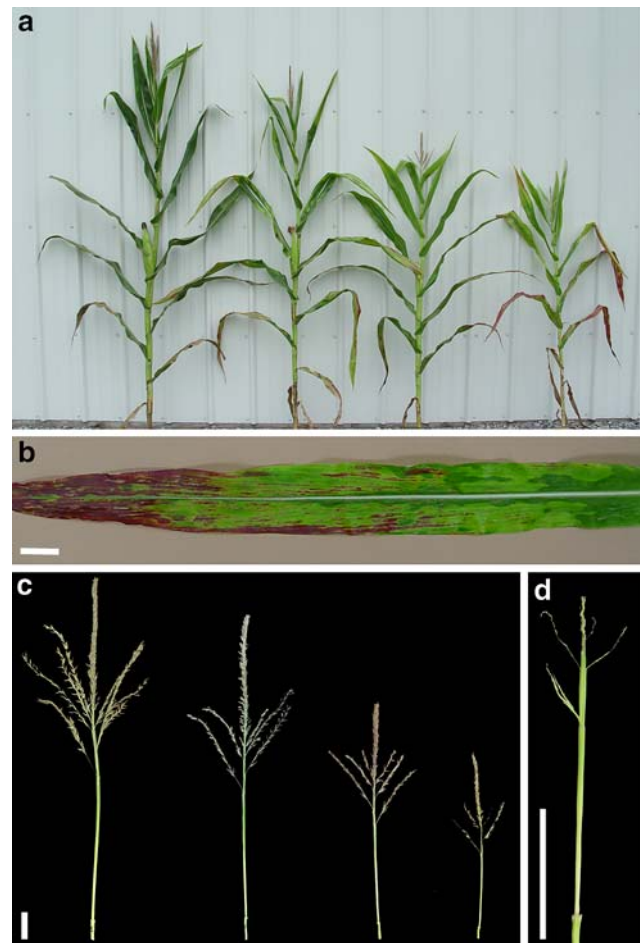


Fig. 4 Phenotypic comparisons among plants from a F₂ family segregating *tdy1-R* and *sxd1-1* mutants. In **a** and **c** the order from left to right corresponds to wild type, *tdy1-R*, *sxd1-1*, and *tdy1-R*; *sxd1-1* double mutant. **a** Double mutants show the greatest reduction in plant height compared with either single mutants or wild-type siblings. **b** Double mutant leaves are severely chlorotic with lighter green tissues restricted to the leaf base. Distinct borders between the chlorotic and green tissues characteristic of *tdy1-R* are visible at the leaf base. The strong tip to base chlorosis gradient of *sxd1-1* expression is evident. **c** Tassel height is most strongly reduced in *tdy1-R*; *sxd1-1* double mutants compared with *sxd1-1* and *tdy1-R* single mutants or wild-type siblings. **d** Approximately half of the *tdy1-R*; *sxd1-1* double mutant plants produced barren tassels lacking spikelets. Scale bars represent 4 cm

display stronger growth retardation than either single mutant.

Since double mutants have more extensive chlorosis in their leaves, we ascertained whether the callose deposits at the vascular parenchyma-bundle sheath cell interface observed in *sxd1-1* single mutants were more severe in the double mutants. Using aniline blue fluorescence, the double mutants showed no enhancement of the callose deposition phenotype and appeared similar to *sxd1-1* single mutants (Fig. 2c, e). Similarly using TEM, we found blockages over the plasmodesmata on the bundle sheath cell side of the bundle sheath–vascular parenchyma cell interface of minor

Table 2 Morphometric analyses in F₂ families

Phenotype	Plant height	wt%	Tassel length	wt%	Anthesis	Ears (%)
Wild type	220.4 ^a ± 0.39	100	55.2 ^a ± 0.14	100	71.9 ^a ± 0.06	100
<i>tdy1-R</i>	196.8 ^b ± 0.92	89.2	47.9 ^b ± 0.28	86.8	80.3 ^b ± 0.13	100
<i>sxd1-1</i>	168.9 ^c ± 1.24	76.6	39.3 ^c ± 0.18	71.2	80.3 ^b ± 0.09	81
<i>tdy1-R; sxd1-1</i>	142.2 ^d ± 0.79	64.5	26.8 ^d ± 0.34	48.6	84.9 ^c ± 0.13	53

Values are the means ± SE. Plant height and tassel length are measured in cm. Anthesis is measured as the number of days after planting until first pollen shed. Percent ears indicates the frequency each phenotypic class produced an ear. Different letters in superscript within a column denote statistical significance determined using Student's *t* test

veins in the double mutants comparable to what we observed in *sxd1-1* single mutant leaves (Fig. 3b, d). In neither case was there any increase in the severity of the phenotype. Hence, *tdy1-R* and *sxd1-1* do not display a synergistic interaction as the double mutant leaves express both single mutant phenotypes. Rather, these data suggest that the phenotypes observed in the double mutants are additive, and that the genes act in independent pathways.

Leaf tips of double mutant plants have the greatest reduction in chlorophyll levels

tdy1-R and *sxd1-1* single mutants both show variegated chlorotic regions in their leaves (Fig. 1b, c). We quantified total chlorophyll levels to determine whether the double mutants were more strongly affected than either single mutant (Table 3). We observed a decreasing series in chlorophyll content with the strongest reduction in the tips of double mutant leaves < the chlorotic regions of either *tdy1-R* or *sxd1-1* single mutant leaves < the green base of *sxd1-1* or double mutant leaves < green regions of *tdy1-R* mutants or wild-type leaves. The leaf bases of *sxd1-1* mutants and the double mutants displayed a mild chlorosis phenotype with approximately 70% as much chlorophyll as wild-type leaves indicating that these tissues are affected by the *sxd1-*

1 mutation. As the tips of double mutant leaves showed a more severe chlorosis phenotype than either single mutant, it suggests that *Tdy1* and *Sxd1* function in separate pathways.

Sugar accumulation in double mutant leaves is greater than in either single mutant

Both single mutants accumulate excess starch in the chlorotic regions of their leaves (Fig. 1e, f). To investigate whether *Tdy1* and *Sxd1* act in the same or separate genetic pathways limiting carbohydrate accumulation in leaves, we determined the starch and soluble sugars content in different phenotypic regions of F₂ plants (Fig. 5; Table S1 in electronic supplementary material). For both the green regions and the chlorotic regions, we found that the double mutants contained similar amounts of starch as the single mutants. In contrast, we determined that the levels of soluble sugars differed with respect to genotype and phenotype. As previously reported, we found green regions of *tdy1-R* leaves had sucrose, glucose and fructose levels indistinguishable from wild type (Braun et al. 2006). However, green leaf bases of the double mutants and *sxd1-1* single mutants contained approximately fourfold higher levels of glucose and fructose as wild type or *tdy1-R* green tissues. Among the chlorotic leaf tissues, the double mutant leaf tips had the highest concentrations of sugars, with approximately 33% greater amounts of glucose, and a significant increase in sucrose content compared with either single mutant. Double mutant leaf tips also contained ~30% more fructose than *sxd1-1* leaf tips and approximately two-fold greater levels than in *tdy1-R* chlorotic regions. Overall, sugar concentrations in green tissues of double mutant leaves are more similar to *sxd1-1* leaf bases than to *tdy1-R* green regions, whereas in chlorotic tissues, the double mutants contain more soluble sugars than either single mutant. Because the double mutants show greater individual sugar accumulation than either single mutant, these data support the hypothesis that *Tdy1* and *Sxd1* function in independent pathways promoting carbon export from leaves.

Table 3 Chlorophyll quantification in F₂ plants

Phenotype	Chlorophyll
Wild type	55.7 ^a ± 0.55
<i>tdy1-R</i> green	54.8 ^a ± 0.57
<i>sxd1-1</i> green	41.0 ^b ± 0.75
<i>tdy1-R; sxd1-1</i> green	42.2 ^b ± 0.67
<i>tdy1-R</i> chlorotic	20.9 ^c ± 0.62
<i>sxd1-1</i> chlorotic	21.5 ^c ± 0.66
<i>tdy1-R; sxd1-1</i> chlorotic	11.4 ^d ± 0.64

Chlorophyll levels were measured in different phenotypic (green or chlorotic) tissues from different genotypes. Values represent the means ± SE in relative units (*n* = 30). Statistical significance was determined using Student's *t* test and indicated by different letters in superscript

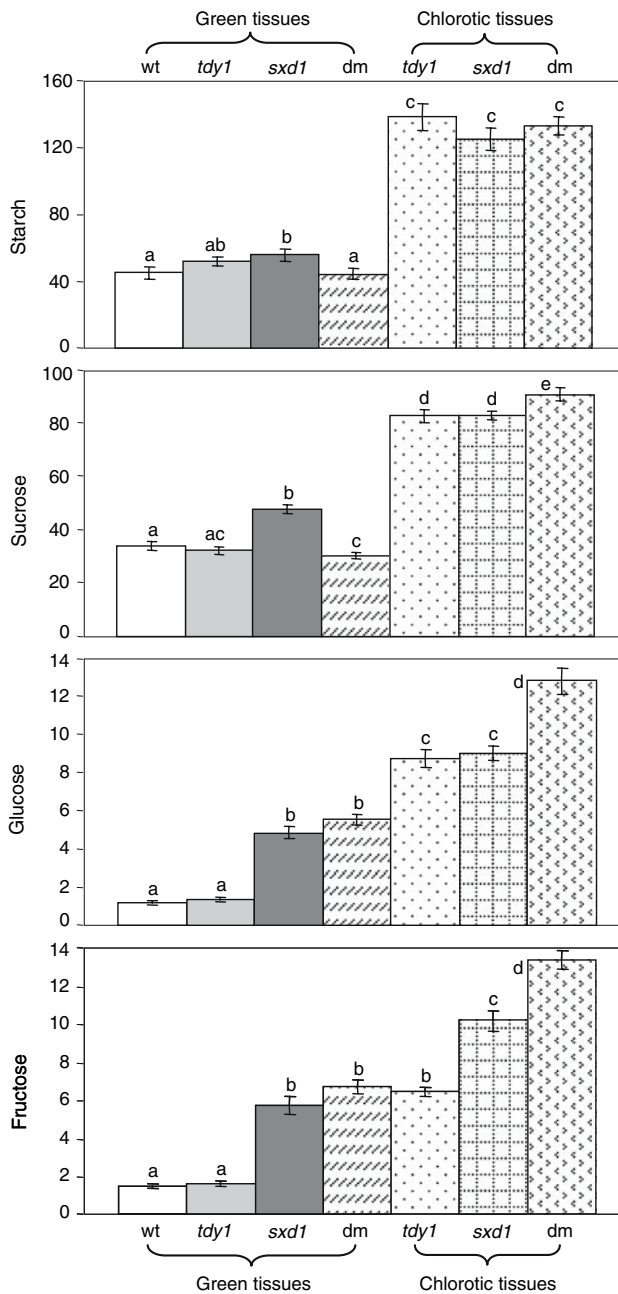


Fig. 5 Carbohydrate quantification in leaves of wild-type, *tdy1-R*, *sxd1-I* and double mutant plants. Units for all panels are mg carbohydrate/g fresh weight. Values are the means of 18 samples ± SE. Abbreviations are wt, wild-type, dm, *tdy1-R*; *sxd1-I* double mutant. Different letters indicate statistically significant differences between samples determined using Student's *t* test

Tdy1 does not function in the same biochemical pathway as *Sxd1*

Sxd1 encodes tocopherol cyclase, the penultimate enzyme in the vitamin E biosynthesis pathway, and *sxd1* mutants lack tocopherols (Sattler et al. 2003). To determine whether *Tdy1* functions in the same biochemical pathway as *Sxd1*,

we quantified tocopherol levels in *tdy1-R* plants (Table 4). We found no statistically significant changes in tocopherol quantities in *tdy1-R* chlorotic or green regions in comparison to wild-type tissue. *sxd1* mutants had undetectable levels of tocopherols as previously reported (Sattler et al. 2003). Hence, *tdy1-R* does not have a lesion in tocopherol synthesis or accumulation, and *Tdy1* does not function in the same biochemical pathway as *Sxd1*.

Discussion

Tdy1 and *Sxd1* independently promote carbon export in maize leaves

tdy1 and *sxd1* are the only known mutations in plants that confer a variegated leaf phenotype with sectors that hyperaccumulate carbohydrates. Using a combination of biochemical, cytological and genetic analyses we investigated whether *Tdy1* and *Sxd1* act in a common pathway. Whereas *sxd1* mutants lack tocopherol, we determined that *tdy1-R* mutants accumulate wild-type levels of tocopherols. Therefore, *Tdy1* does not function in the same biochemical process as *Sxd1*. *sxd1* mutants accumulate carbohydrates in leaf tissues due to callose being deposited over the interface of bundle sheath-vascular parenchyma cells in leaf minor veins which blocks sucrose symplastic movement. Using aniline blue fluorescence microscopy we did not identify any ectopic callose deposition in *tdy1-R* mutant leaf tissues. Moreover, using TEM we did not observe any structural alterations to the plasmodesmata, indicating that the symplastic loading pathway is not physically impeded. This suggests that *tdy1-R* mutants do not accumulate carbohydrates due to an occlusion, but rather due to a different cellular mechanism. This was confirmed by double mutant analyses which showed that the two mutations had an additive interaction. We found that the double mutants expressed both single mutant leaf phenotypes, that the reductions in plant height, tassel size and chlorophyll levels were additive, and that the accumulation of sugars in chlorotic leaf tissues of the double mutants was greater than in either single mutant. In addition, half of the double mutants produced ears whereas the *tdy1-R* mutant frequency was indistinguishable from wild type and 81% of the *sxd1-I* single mutants made ears. The increased frequencies in the failure to make ears and production of barren tassels observed in the double mutants are most likely explained by an additive retention of carbohydrates in leaf tissues and a concomitant failure to export sucrose to the developing inflorescences. Collectively, these data lead us to conclude that *Tdy1* and *Sxd1* function independently, and that *tdy1* defines a distinct genetic pathway affecting carbon partitioning in maize leaves.

Table 4 Tocopherol quantification

Phenotype	Tocopherol
Wild type	118.6 ^a ± 3.59
<i>tdy1-R</i> green	101.0 ^a ± 3.17
<i>tdy1-R</i> chlorotic	112.3 ^a ± 6.17
<i>sxd1-1</i>	nd

Values are means of six samples ± SE measured in µg/g fresh weight. *nd* indicates none detected. Values indicated by letter “a” in superscript were not statistically different as determined using Student’s *t* test

Chlorotic leaf tissues do not retain sink identity

We previously suggested that one possibility to explain the excess carbon accumulation in *tdy1-R* chlorotic leaf sectors was a block in the developmental transition from sink to source identity, such that the chlorotic sectors continued to import photoassimilates from neighboring green tissues (Braun et al. 2006). If the chlorotic tissues were to remain sinks, the large amounts of green source tissues could potentially provide the carbohydrates accumulating in the chlorotic regions. However, based on our genetic analyses, our data do not support this hypothesis. In the *tdy1-R*; *sxd1-1* double mutants, the amount of green leaf tissue is greatly reduced and is restricted to a narrow region at the very base of the leaves. Additionally, this green tissue displays mild chlorosis and an increase in carbohydrate accumulation indicating that it is perturbed in carbon export. As this tissue is proximal to and up to a meter distant from the chlorotic tip of adult leaves, it is highly unlikely to be providing the carbohydrates that accumulate in the cells near the tip. Furthermore, half of the double mutant plants produced a tassel and an ear. These are sink tissues dependent on the photosynthetic source leaves for their carbohydrates. Because the great majority of the area of double mutant leaves is severely chlorotic, yet still must be capable of exporting photoassimilates to produce the developing reproductive tissues, our data argues against the chlorotic tissues remaining sinks and does not support the hypothesis that *Tdy1* functions to regulate the sink to source transition. Rather, the new data lead us to favor the hypothesis that the cells in the *tdy1* chlorotic region are source tissues that are partly blocked in carbon export capacity.

A model for TDY1 function

In wild-type maize leaves, sucrose is synthesized in mesophyll cells, diffuses through plasmodesmata into bundle sheath cells and then into the vascular parenchyma cells (Fig. 6a). Sucrose is exported from the vascular parenchyma cell to the apoplast, and then loaded into the phloem by sucrose transporters in the plasma membrane of the companion cell and/or sieve element (Lalonde et al. 2004;

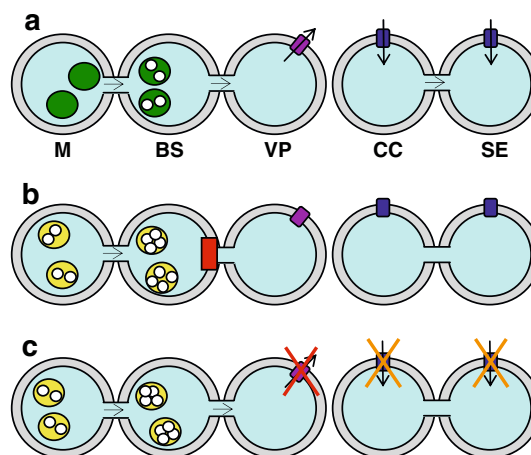


Fig. 6 Model for TDY1 functions in phloem loading of sucrose. Diagrams represent the pathway of sucrose movement from photosynthetic cells into the phloem. *M* mesophyll, *BS* bundle sheath, *VP* vascular parenchyma, *CC* companion cell, *SE* sieve element. *Green* and *yellow* ovals in *M* and *BS* cells represent chloroplasts. *White circles* within chloroplasts represent starch grains. *Magenta box* on *VP* plasma membrane represents sucrose efflux transporter, and *blue boxes* on *CC* and *SE* plasma membranes depict sucrose transporters. *Arrows* indicate the direction of sucrose movement. **a** Wild-type tissue with normal, unimpeded sucrose movement into the phloem. **b** *sxd1-1* mutant chlorotic tissue has callose deposits (*red box*) over the plasmodesmata at the *BS*–*VP* cell interface blocking sucrose movement and resulting in carbohydrate accumulation in *M* and *BS* cells. **c** *tdy1-R* chlorotic tissue has normal appearing plasmodesmata and lacks callose deposits. We hypothesize that either the sucrose efflux transport step is inhibited (*red X*) or the *CC*–*SE* sucrose transporters (*orange X*) fail to load sucrose into the phloem. This would result in the carbon hyperaccumulation observed in the photosynthetic cells

Sauer 2007). *sxd1* mutant leaf tips are blocked in this pathway at the bundle sheath–vascular parenchyma cell interface (Fig. 6b) (Russin et al. 1996; Botha et al. 2000; Provencher et al. 2001).

tdy1 chlorotic sectors accumulate excess carbohydrates indicating that they have a defect in phloem loading. In agreement with this, we previously localized the site of TDY1 function to the innermost tissue layer of leaves comprised of the veins, bundle sheath cells, and interveinal mesophyll cells (Baker and Braun 2007). Due to the limits of the experiment it was not possible to further delineate where within this tissue layer TDY1 acts. However, the cytological investigations presented resolve this ambiguity. As we observed no blockages or alterations to plasmodesmatal structure along the sucrose symplastic pathway in *tdy1-R* leaves, the carbon accumulation points to a defect at a later step in phloem loading. Nonetheless, even though the plasmodesmata appear unobstructed, we cannot be certain that they are functional. However, we propose that a molecular blockage of plasmodesmata precluding sucrose movement is an unlikely scenario for the following reason. In *sxd1* mutants, specific plasmodesmata are occluded and unable to transit sucrose, causing the vascular parenchyma

cells to appear plasmolysed due to their low osmotic concentration (Russin et al. 1996). Accordingly, we carefully inspected for, but never observed, plasmolysis of any vascular parenchyma, mesophyll or bundle sheath cells in *tdy1* mutants in our microscopic analyses. Therefore, these data suggest that sucrose is able to pass freely between cells along the symplastic pathway, and hence that TDY1 likely functions in the veins (Fig. 6c).

From the variegated phenotype of *tdy1* mutants, we hypothesize that TDY1 acts as a regulator of sucrose transport rather than as a transporter itself, as loss of transporter function leads to uniform carbohydrate accumulation and chlorosis phenotypes (Riesmeier et al. 1994; Burkle et al. 1998; Gottwald et al. 2000; see Braun et al. 2006; Baker and Braun 2007 for discussion of mechanisms for *tdy1* variegation). Several possibilities are envisioned for *Tdy1* function. The first possibility is that *Tdy1* may regulate sucrose efflux out of vascular parenchyma cells. Failure to export sucrose to the apoplast would create a bottleneck restriction leading to the build-up of sucrose in the vascular parenchyma cells and, in turn, to carbohydrate accumulation in the bundle sheath and mesophyll cells. The second possibility is that *Tdy1* may function to regulate the activity of the H⁺-ATPases or sucrose transporters within the companion cells and sieve elements. Lack of function of either the H⁺-ATPases or sucrose transporters results in failure to load sucrose into the phloem and thereby to excess accumulation in the apoplast. Sucrose accumulation in the apoplast would shift the equilibrium for sucrose export from vascular parenchyma cells leading to increased concentration within these cells, and ultimately to carbon accumulation in the photosynthetic cells. In support of this, antisense expression or mutation of a phloem H⁺-ATPase or sucrose transporters causes an accumulation of carbohydrates in photosynthetic cells and chlorosis (Riesmeier et al. 1994; Burkle et al. 1998; Gottwald et al. 2000; Zhao et al. 2000). A third possibility is that TDY1 may function in the sucrose signal transduction pathway that regulates the abundance of the sucrose transporter controlling phloem loading (Chiou and Bush 1998; Vaughn et al. 2002; Ransom-Hodgkins et al. 2003).

Our analyses of the *tdy1-R* mutant phenotype and genetic interactions between *tdy1-R* and *sxd1-1* have shown that *Tdy1* acts independently of *Sxd1*. Thus, the *tdy1* mutation identifies a separate genetic pathway limiting carbon accumulation in maize leaves. Future work characterizing the molecular function of *Tdy1* will determine the mechanism by which *Tdy1* influences carbon partitioning. Understanding the control of carbon export from leaves will lead to novel strategies to manipulate carbon allocation and biomass deposition which may have applications in the production of biofuels.

Acknowledgments This work was supported by the National Research Initiative of the United States Department of Agriculture Cooperative State Research, Education and Extension Service, grant number 2004-35304-14948 to D.M.B. We thank Tony Omeis and Scott Harkcom for excellent plant care. We also thank Laurel Mezitt Provencher for the gift of the *sxd1-1* stock. We thank three anonymous reviewers, Simon Gilroy and members of the Braun and McSteen labs for discussion of the data and comments on the manuscript.

References

- Aoki N, Hirose T, Takahashi S, Ono K, Ishimaru K, Ohsugi R (1999) Molecular cloning and expression analysis of a gene for a sucrose transporter in maize (*Zea mays* L.). *Plant Cell Physiol* 40:1072–1078
- Baker RF, Braun DM (2007) *tie-dyed1* functions non-cell autonomously to control carbohydrate accumulation in maize leaves. *Plant Physiol* 144:867–878
- Botha CEJ, Cross RHM, van Bel AJE, Peter CI (2000) Phloem loading in the sucrose-export-defective (*SXD-1*) mutant maize is limited by callose deposition at plasmodesmata in bundle sheath–vascular parenchyma interface. *Protoplasma* 214:65–72
- Braun DM, Ma Y, Inada N, Muszynski MG, Baker RF (2006) *tie-dyed1* regulates carbohydrate accumulation in maize leaves. *Plant Physiol* 142:1511–1522
- Burkle L, Hibberd JM, Quick WP, Kuhn C, Hirner B, Frommer WB (1998) The H⁺-sucrose cotransporter NtSUT1 is essential for sugar export from tobacco leaves. *Plant Physiol* 118:59–68
- Bush D (1993) Proton-coupled sugar and amino acid transporters in plants. *Annu Rev Plant Physiol Plant Mol Biol* 44:513–542
- Chiou TJ, Bush DR (1998) Sucrose is a signal molecule in assimilate partitioning. *Proc Natl Acad Sci USA* 95:4784–4788
- Dinges JR, Colleoni C, Myers AM, James MG (2001) Molecular structure of three mutations at the maize *sugary1* locus and their allele-specific phenotypic effects. *Plant Physiol* 125:1406–1418
- Esau K (1977) *Anatomy of seed plants*. Wiley, New York
- Evert RF, Eschrich W, Heyser W (1978) Leaf structure in relation to solute transport and phloem loading in *Zea mays* L. *Planta* 138:279–294
- Fisher D, Eschrich W (1985) Import and unloading of ¹⁴C assimilate into nonphotosynthetic portions of variegated *Coleus blumei* leaves. *Can J Bot* 63:1708–1712
- Gaxiola RA, Palmgren MG, Schumacher K (2007) Plant proton pumps. *FEBS Lett* 581:2204–2214
- Goldschmidt EE, Huber SC (1992) Regulation of photosynthesis by end-product accumulation in leaves of plants storing starch, sucrose, and hexose sugars. *Plant Physiol* 99:1443–1448
- Gottwald JR, Krysan PJ, Young JC, Evert RF, Sussman MR (2000) Genetic evidence for the *in planta* role of phloem-specific plasma membrane sucrose transporters. *Proc Natl Acad Sci USA* 97:13979–13984
- Hofius D, Hajirezaei M-R, Geiger M, Tschiersch H, Melzer M, Sonnewald U (2004) RNAi-mediated tocopherol deficiency impairs photoassimilate export in transgenic potato plants. *Plant Physiol* 135:1256–1268
- Hofstra G, Nelson C (1969) The translocation of photosynthetically assimilated ¹⁴C in corn. *Can J Bot* 47:1435–1442
- Jeannette E, Reyss A, Gregory N, Gantet P, Prioul JL (2000) Carbohydrate metabolism in a heat-girdled maize source leaf. *Plant Cell Environ* 23:61–69
- Krapp A, Stitt M (1995) An evaluation of direct and indirect mechanisms for the “sink-regulation” of photosynthesis in spinach: changes in gas exchange, carbohydrates, metabolites, enzyme

- activities and steady-state transcript levels after cold-girdling source leaves. *Planta* 195:313–323
- Lalonde S, Wipf D, Frommer WB (2004) Transport mechanisms for organic forms of carbon and nitrogen between source and sink. *Annu Rev Plant Biol* 55:341–372
- Lunn JE, Furbank RT (1999) Tansley review no. 105: sucrose biosynthesis in C₄ plants. *New Phytol* 143:221–237
- Madore MA (1990) Carbohydrate metabolism in photosynthetic and nonphotosynthetic tissues of variegated leaves of *Coleus blumei* Benth. *Plant Physiol* 93:617–622
- Maeda H, Song W, Sage TL, DellaPenna D (2006) Tocopherols play a crucial role in low-temperature adaptation and phloem loading in *Arabidopsis*. *Plant Cell* 18:2710–2732
- Provencher LM, Miao L, Sinha N, Lucas WJ (2001) *Sucrose export defective1* encodes a novel protein implicated in chloroplast-to-nucleus signaling. *Plant Cell* 13:1127–1141
- Ransom-Hodgkins W, Vaughn M, Bush D (2003) Protein phosphorylation plays a key role in sucrose-mediated transcriptional regulation of a phloem-specific proton-sucrose symporter. *Planta* 217:483–489
- Rhoades M, Carvalho A (1944) The function and structure of the parenchyma sheath plastids of the maize leaf. *Bull Torrey Bot Club* 71:335–346
- Riesmeier JW, Willmitzer L, Frommer WB (1994) Evidence for an essential role of the sucrose transporter in phloem loading and assimilate partitioning. *EMBO J* 13:1–7
- Russin WA, Evert RF, Vanderveer PJ, Sharkey TD, Briggs SP (1996) Modification of a specific class of plasmodesmata and loss of sucrose export ability in the *sucrose export defective1* maize mutant. *Plant Cell* 8:645–658
- Ruzin S (1999) *Plant Microtechnique and Microscopy*, Oxford University Press, New York
- Sattler SE, Cahoon EB, Coughlan SJ, DellaPenna D (2003) Characterization of tocopherol cyclases from higher plants and cyanobacteria. Evolutionary implications for tocopherol synthesis and function. *Plant Physiol* 132:2184–2195
- Sauer N (2007) Molecular physiology of higher plant sucrose transporters. *FEBS Lett* 581:2309–2317
- Scofield GN, Aoki N, Hirose T, Takano M, Jenkins CLD, Furbank RT (2007) The role of the sucrose transporter, OsSUT1, in germination and early seedling growth and development of rice plants. *J Exp Bot* 58:483–495
- Sheen J (1990) Metabolic repression of transcription in higher plants. *Plant Cell* 2:1027–1038
- Spurr A (1969) A low-viscosity epoxy resin embedding medium for electron microscopy. *J Ultrastruct Res* 26:31–43
- Vaughn MW, Harrington GN, Bush DR (2002) Sucrose-mediated transcriptional regulation of sucrose symporter activity in the phloem. *PNAS* 99:10876–10880
- Yu F, Fu A, Aluru M, Park S, Xu Y, Liu H, Liu X, Foudree A, Nambogga M, Rodermeier S (2007) Variegation mutants and mechanisms of chloroplast biogenesis. *Plant Cell Environ* 30:350–365
- Zhao R, Dielen V, Kinet J-M, Boutry M (2000) Cosuppression of a plasma membrane H⁺-ATPase isoform impairs sucrose translocation, stomatal opening, plant growth, and male fertility. *Plant Cell* 12:535–546